Counterion induced bundle formation of rodlike polyelectrolytes

ARTICLE *in* BERICHTE DER BUNSENGESELLSCHAFT/PHYSICAL CHEMISTRY CHEMICAL PHYSICS · JUNE 1996

DOI: 10.1002/bbpc.19961000620

Counterion Induced Bundle Formation of Rodlike Polyelectrolytes

Jay X. Tang, Shuen Wong, Phong T. Tran*), and Paul A. Janmey

Division of Experimental Medicine, Brigham and Women's Hospital, 221 Longwood, Av., LMRC301, Boston, MA 02115, USA

Key Words: Biophysical Chemistry / Biopolymers / Clusters / Light, Scattering / Phase Transitions

A number of filamentous biopolymers including actin filaments (F-actin), microtubules (MT), tobacco mosaic virus (TMV), and the filamentous bacteriophage *fd* form bundles under well-defined conditions. All of these macromolecules are negatively charged rodlike assemblies, and lateral association is induced by a number of cations such as divalent and trivalent metal ions and homopolymers of basic peptides. The general features of bundle formation are largely independent of the specific structure of the biopolymers and the bundling agent used. They are also approximately independent of the concentration of macromolecules. However, a threshold concentration of bundling agent is required in order to form large lateral aggregates, detected by a sharp increase in light scattering and by electron microscopy. The threshold concentration varies strongly with the valence of the cations and increases with the ionic strength of the solution. The formation of bundles is reversible by polyanions such as nucleoside phosphates. This overall behavior is similar to the phenomenon of DNA condensation and can be explained by applying polyelectrolyte theories, including the concept of counterion condensation. Our results provide quantitative comparisons with a number of predictions of polyelectrolyte theories, including the calculation of apparent binding affinity and its dependence on ionic strength. They also support the prediction of an attractive interaction between the neighboring filaments due to sharing of counterion clouds. In addition, the simply detectable, reversible assembly of macromolecules in solution serves as a sensitive indicator of the active association of small ions and the formation of ion clusters. Association constants of $Co(NH_3)_6^{3+}$-ATP and Lys_{18}-ATP were determined by application of this model.

1. Introduction

Nature has provided a variety of charged macromolecules for testing the theory of polyelectrolytes. These biopolymers include DNA, cytoskeletal filaments such as F-actin and microtubules (MT), and viruses like tobacco mosaic virus (TMV) and filamentous bacteriophage fd. They all appear to be rodlike particles, although with different length, diameter, and internal stiffness. Since these biopolymers are assembled from many identical subunits with well determined molecular composition and a high level of packing geometry, the charge distribution of these assemblies can be reliably predicted and modeled. It is therefore useful to conduct experimental studies on all of these systems and select different aspects for quantitative comparisons with theory.

Polyelectrolyte properties of DNA have been most widely studied, and the original counterion condensation theory of linear polyelectrolytes has been successfully applied to explain the phenomenon of DNA condensation [1–4]. A double stranded DNA at neutral pH has a linear charge spacing $b = 1.7$ Å, much less than the Bjerrum length $\lambda_B = e^2/4\pi\varepsilon_0\varepsilon kT$ ($\lambda_B = 7.1$ Å with the dielectric constant $\varepsilon = 80$ in water at 20 °C). According to the Manning counterion condensation theory, a consequence of DNA's high charge density is that a certain fraction of its charge is neutralized due to the territorial binding of counterions in the immediate environment. The charge fraction of the condensed ions is determined as

$$\Theta = \left(1 - \frac{1}{N\xi}\right), \qquad (1)$$

where N is the valence of the counterion and $\xi = \lambda_B/b = 4.2$. In monovalent electrolyte, θ is calculated to be 76%; while $\theta = 88\%$ in the presence of sufficient divalent cations. The predicted delocalized binding is stronger for counterions of higher valence, in which case the charged polymer is neutralized to a higher degree as shown in Eq. (1).

The residual electrostatic repulsion between the DNA molecules of like charge tends to keep them apart. This repulsive force decreases with the presence of polyvalent counterions, due to the enhanced charge condensation. In addition, an attractive interaction can be induced by the two DNA molecules sharing counterions. The lateral redistribution [4] and the longitudinal fluctuation [5] of the counterions have each been shown in theory to cause an attractive interaction between polyelectrolytes. Therefore at appropriate ionic conditions, a balance between attractive and repulsive interactions can be reached so that the filaments in suspension can get close enough to form stabilized aggregates. The eventual formation may also involve other interactions such as hydration and Van der Waals force [1, 3]. It has been estimated that DNA condensation occurs as θ reaches 90%. Therefore, a valence of three or higher is required for DNA condensation, or alternatively, divalent cations at special solution conditions such as the presence of ethanol to reduce the dielectric constant ε, or PEG to increase osmotic pressure of the system.

Although the counterion condensation theory initially assumed the polyelectrolyte to be infinitely long, straight, and thin, the theory has been successfully applied to several real, less ideal systems in addition to DNA. Analytical solutions to the nonlinear Poisson-Boltzmann equation for a cylindrical polyelectrolyte [6, 7] provide a model generally consistent with that of the earlier counterion condensation theory. Various other theoretical approaches arrive at similar predictions, which are further supported by Monte Carlo simulations [8, 9]. In this paper, we choose to apply

*) Biology Department, University of North Carolina, Chapel Hill, NC 27599

the much simplified predictions from the original Manning theory to explain the mechanism of the bundle formation of rodlike polyelectrolytes.

Cytoskeletal filaments such as F-actin and microtubules have been extensively studied because of their important functional roles in cells [10]. F-actin, for example, has long been observed to form large lateral aggregates in the presence of various divalent or trivalent metal ions [11, 12], polyamines such as spermine and spermidine [13], and a number of other polyvalent cations [14, 15]. However, very little emphasis in the past was put on explaining the mechanism of these formations, in spite of the striking similarity between such phenomenon and DNA condensation. Furthermore, although a long list of proteins have been shown to bind and bundle F-actin, many of them appear to lack a common and specific binding site on the surface of actin filaments. Instead, the common basic nature of many of the proteins in this class suggests a formation that is driven in general by charge neutralization. The essential goal of this paper is to establish the mechanism of such bundle formations based on an analogy with DNA condensation.

Rodlike viruses such as tobacco mosaic virus (TMV) and filamentous bacteriophage fd provide unique advantage to the study of bundle formation. They are extremely stable in a wide range of salt concentration, allowing the study of ionic strength dependence over several orders of magnitude. The viruses of each kind are identical in physical parameters such as length, diameter, internal stiffness, and linear charge density. X-ray scattering studies have determined within atomic resolution the molecular packing of these viruses. Because of their ideal properties and well developed preparation methods, both viruses have been extensively studied as model systems for lyotropic liquid crystalline formations [16, 17]. In addition, TMV gels have been previously studied by X-ray scattering to determine the interrod forces between charged cylinders [18, 19].

We report in this paper the bundle formations of F-actin, MT, fd, and TMV. The common features among these systems provide experimental evidence that the lateral association of these particles is driven by the same process of counterion condensation. Such a process requires the presence of polyvalent cations to reach a certain threshold concentration. The difference in threshold among these systems is mainly related to the different diameter and surface charge among the macromolecules. Since the apparent binding of the polycations weakens with increasing monovalent salt in solution, a simple increase of salt may reverse the bundle formation. This prediction based on the counterion condensation theory can be tested quantitatively using systems such as fd and TMV.

Bundle formation of rodlike polyelectrolytes is also reversible by addition of polyanions. We hypothesize that polyanions in general form ion clusters with polycations and hence deplete the concentration of free polycations to below a threshold concentration required to sustain lateral association. The bundles therefore disassemble into separate filaments. They may reform when more polycations are added, and the process may continue. Through many cycles of such processes, it should be possible to obtain the association constant between the test polyions, using only a trace amount of charged macromolecules as an indicator. This is because the light scattering signal is extremely sensitive to the aggregation of the macromolecules in solution. In this report, association constants of $Co(NH_3)_6^{3+}$-ATP and Lys_{18}-ATP are obtained by application of the ion cluster model.

2. Experimental

2.1 Materials

Monomeric (G-)actin was purified according to the method of Spudich and Watt [20]. The nonpolymerizing buffer contained 4 mM hepes adjusted to pH 7.5, 0.2 mM $CaCl_2$, 0.5 mM ATP, and 0.5 mM NaN_3. F-actin was polymerized from G-actin by 150 mM KCl.

Tubulin was purified using the method of Voter and Erickson [21]. The final suspension contained 100 mM pipes at pH 6.9, 1 mM EGTA, 1 mM $MgSO_4$, and 0.5 mM GTP (PEM buffer). The concentration of the tubulin was determined using the BioRad dye-binding assay, with BSA as a standard. For the light scattering study, 10 mg/ml stock tubulin was allowed to spontaneously assemble into microtubules (MTs) at 37 °C, and the MTs were stabilized with 10 μM taxol to prevent depolymerization. Under this assembly condition, MTs can reach lengths exceeding hundreds of microns. We subjected the long MTs to a 5 s pulse of high frequency sonication to break them into short fragments. The stabilized MTs were further diluted with PEM buffer to the final concentrations used in this study. 10 μM taxol was also contained in the dilution buffer to prevent the depolymerization of MTs through the measurements.

TMV was purified in the lab of D.L.D. Caspar at the Rosenstiel Basic Medical Research Center of Brandeis University [22]. fd, a close relative of M13, was prepared similarly in the same lab by a standard method [23]. Both virus suspensions were kept in 5 mM Tris at pH 7.5 and 1 mM NaN_3. The virus particles usually remain intact for a long period of time at 4° C.

Human plasma gelsolin was purified by elution from DE-52 ion exchange matrix in 30 mM NaCl, 3 mM $CaCl_2$, 25 mM Tris pH 7.4 as described by Kurokawa et al. [24], rapidly frozen in liquid nitrogen and stored at −80 °C.

Concentrations of virus suspensions and proteins, with the exception of tubulin, were determined by optical absorbance. The following extinction coefficients were used: fd: 3.84 ml mg^{-1} cm^{-1} at 269 nm, TMV: 3.05 ml mg^{-1} cm^{-1} at 280 nm, G-actin: 0.63 ml mg^{-1} cm^{-1} at 290 nm, and gelsolin: 1.8 ml mg^{-1} cm^{-1} at 280 nm.

Oligomers of arginine and histidine were synthesized and purified at the Latvian Organic Synthesis Institute and were a generous gift of Rolands Vegners. Polylysine of average degree of polymerization approximately 18, noted as Lys_{18}, was purchased from Sigma. All the other common chemicals are of research or analytical grade.

2.2 Methods

90° light scattering experiments were performed with a Perkin-Elmer LS-5B luminescence spectrometer. The incident wavelength was set to 365 nm (3 nm slit) and the scattered light was detected at 375 nm (3 nm slit) in order to reduce the signal level. Different settings were sometime used but were found inconsequential for our study, since we were only interested in detecting changes in scattering. However, comparison of light scattering readings in each plot was always made at a fixed instrumental setting. A typical rectangular light scattering cuvette of 10 nm path length and 5 mm width takes 600 microliters of solution. When a concentrated stock of reagent was sequentially added into the sample cuvette, special care was taken so that the eventual effect of dilution was less than 5% and was hence neglected. Since many cycles of additions were necessary in order to obtain the data of Figs. 6, 7, and 8, larger sample volumes of 2 ml were used, held by square cuvettes.

Electron micrographs were obtained through a JEOL 1200-EX transmission electron microscope, using the conventional negative staining technique. The specimens were viewed and photographed at either 80 kV (for fd), or 100 kV (for F-actin).

3. Results

3.1 Reversible Formation of Polyelectrolyte Bundles

Static light scattering and negative staining electron microscopy (EM) provide an ideal combination of experimental techniques in the detection of lateral association of macromolecules. Biopolymers are large enough to give strong scattering signals with a concentration less than one tenth of a milligram per milliliter, and the scattering signals increase steeply when larger aggregates are formed by lateral association. The measurements cause no disturbance to the sample, allowing convenient examination of different parts of a sample as well as the same sample following repeated operations. An EM preparation requires only microliters of solution and the negative staining procedure takes less than a minute to perform. Despite possible artifacts produced in the staining and drying process, large bundles of protein rich filaments can be readily and unambiguously detected, and the morphologies compared between different samples following the same treatment.

Figure 1 displays the overall effect of a number of polyvalent cations on four types of biopolymers, including F-actin (a), fd (b), microtubules (c), and TMV (d). Actin concentration was 0.5 mg/ml, and the remaining three were 0.3 mg/ml. The slit setting in the light scattering measurements for fd was 5 nm/5 nm as opposed to 3 nm/3 nm for the rest. All the polyvalent cations were added in the form of concentrated chloride salt. A sharp increase in the light scattering signal corresponds to the formation of large lateral aggregates, confirmed by electron microscopy. The list of the cations shown to induce bundle formation is somewhat arbitrary and by no means complete. Nevertheless, it is apparent from Fig. 1 that bundle formation is largely in-

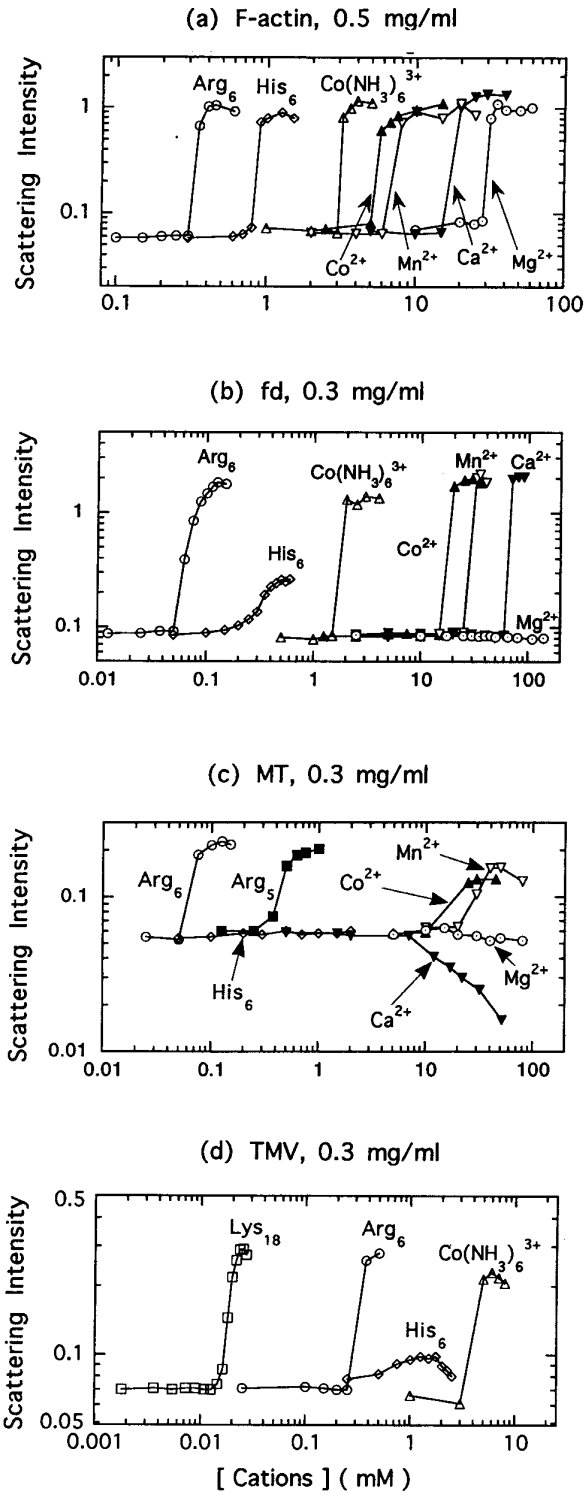

Fig. 1
Light scattering intensity as a function of cation concentration, following sequencial additions of various polycations. A steep increase indicates formation of large lateral aggregates. The susceptibility of bundle formation decreases in the order from (a) F-actin to (b) fd, (c) MT, and (d) TMV. Each bundling agent used is noted close to the respective plot, and same symbol types correspond to same cation species among the four figures

dependent of the specific macromolecular composition or internal structure, but instead, it must be driven by a rather general process.

The general features in Fig. 1 can be explained by the same theory of polyelectrolytes that has been applied to DNA condensation [1 – 3]. All four types of biopolymers can be modeled as charged cylinders whose linear charge densities are in the regime where counterion condensation is expected. Furthermore, an attractive interaction can occur when two cylinders of the same charge get close enough to be able to share the counterion clouds, by either counterion fluctuation [5] or the radial redistribution [4] of the counterions. Since the fraction of charge of counterions in the condensation layer increases with the valence of cations, the residual repulsion between the partially screened cylinders of like charge decreases. Eventually, a balance is reached, and stable lateral aggregates form. This simple picture agrees with the fact that cations of valence of 2 or greater are required to induce bundle formation, and the overall trend that a lower threshold is required for cations of higher valence.

It is informative to compare the relative susceptibility of the bundle formation among the four systems studied, although such a comparison is somewhat obscured by the different salt conditions required to maintain each native state. F-actin was initially in 150 mM KCl in addition to the low ionic strength buffer, MT in 100 mM PIPES, 1 mM EGTA, 1 mM $MgSO_4$, and 0.5 mM GTP. fd and TMV were prepared in 5 mM Tris at pH 7.5 plus 50 and 30 mM KCl, respectively. In general, higher concentrations of polycations are necessary at higher initial ionic strength, which is roughly the concentration of free monovalent salt ions in the above solutions. The ionic strength dependence will be discussed in detail later in this paper. It seems clear that after taking into account the difference in ionic strength, F-actin is more susceptible to bundle formation than fd. F-actin and fd are both much more susceptible to bundling than MT and TMV. TMV requires at least trivalent cations to form bundles, while some common divalent metal ions such as Co^{2+} and Mn^{2+} can induce MT bundles. Ca^{2+} destabilized MT and caused a decrease in the light scattering signal. This specific effect has been recognized for a long time. For instance, micromolar Ca^{2+} has been shown to inhibit the formation of MTs [25]. In our study, MTs are previously formed and stabilized by 10 μM taxol, and they seemed resistant to depolymerization until the concentration of Ca^{2+} was raised to above 5 millimolar.

There is a certain extent of variation among small counterions in the threshold concentration required to form bundles. For instance, Co^{2+} bundles F-actin at 5.5 mM in comparison with Mn^{2+} at 7 mM, Ca^{2+} at 20 mM, and Mg^{2+} at 27 mM. In case of fd in 5 mM Tris buffer and 50 mM KCl, bundle formation requires about 20 mM of Co^{2+}, 30 mM Mn^{2+}, or 70 mM Ca^{2+}. Mg^{2+} of up to 150 mM concentration is incapable of bundling fd filaments. This variation among divalent cations is presumably due to slight differences in the extent of charge neutralization. Such differences are independent of the biopolymer systems used, since the same sequence of onset bundling concentrations occurs for F-actin, fd, and MT. Among the four common divalent metal ions tested, the bundling efficiency increases with their order in the periodic table, suggesting some correlation with their atomic structure including the radius of electron cloud and the extent of hydration in solution.

The effect of histidine hexamers on the bundle formation deserves a special note. This is because histidine has a pK value of 6.5, hence presumably less than half of the residues are protonated to carry positive charges at pH 7.5. Therefore, one would expect His_6 to be a weaker bundle inducer than the trivalent hexamine cobalt ions. In fact, however, it bundles F-actin more efficiently than $Co(NH_3)_6^{3+}$. It also begins to bring fd and TMV filaments together at lower concentrations than that of $Co(NH_3)_6^{3+}$, however, the light scattering signal does not increase to the high level when the bundles form in all other cases. We speculate that different His_6 molecules have various extents of protonation, and since the ones that carry more than three charged residues bundle much more efficiently than $Co(NH_3)_6^{3+}$, the overall onset concentration of bundle formation appears lower than that of $Co(NH_3)_6^{3+}$. It is also possible that His_6 may aggregate to small clusters and the clusters carry enough charges to cause the formation of bundles of the negatively charged biopolymers. But on the other hand, since the protonation of His_6 is rather weak and incomplete, it is not a strong bundler for most of the biopolymers studied. This may explain the unique behavior of His_6 in Fig. 1.

Since sufficient concentrations of free polycations are required to ensure the lateral association, one might expect the possibility of reversing the bundling process by depleting the free polyvalent cations in solution. This idea can be easily tested with polyanions such as common nucleotides, which contain a varying number of negatively charged phosphate groups. Many previous studies reported that millimolar concentrations of ATP dissolved bundles of F-actin which were induced by spermine, spermidine, as well as some basic proteins [13, 26]. Fig. 2 shows the disaggregation of fd bundles by adding respectively di(adenosine-5′)pentaphosphate (AP5A), ATP, ADP, and AMP. The amount of anions required increased with decreasing negative charges. fd concentration was 0.1 mg/ml, and the initial scattering readings were all about 0.05. Bundles of fd were formed by adding Lys_{18} to 50 μM, and the signal level reached about 0.9 prior to additions of nucleotides. Note that submillimolar AP5A and mM ATP disaggregated fd bundles completely. In contrast, the reversal of the same bundle formation by ADP and AMP were incomplete with even much lager amounts.

Fig. 3 provides a visual display of large F-actin and fd bundles and the complete disaggregation by ATP. Each filamentous suspension of 0.1 mg/ml was incubated with 5 mM $Co(NH_3)_6^{3+}$ for a few minutes prior to staining. The EM pictures of bundles were taken at 100000× magnification. 5 mM ATP was then added to each solution, and after mixing, the suspension was subject to the same staining procedure and EM pictures taken at 50000×. Most of the

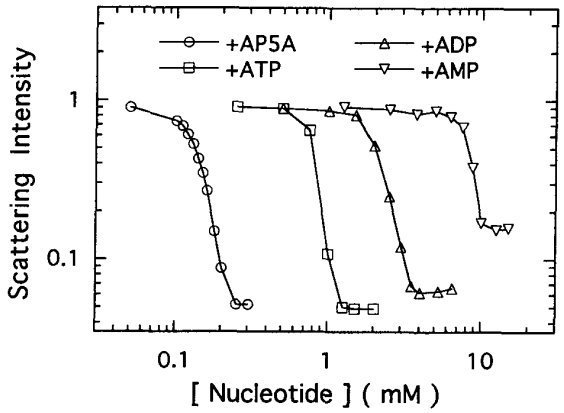

Fig. 2
Decrease of light scattering intensities indicates disaggregation of fd bundles by di(adenosine-5')pentaphosphate (AP5A), ATP, ADP, or AMP. Initial solutions of 0.1 mg/ml fd in 5 mM Tris and 50 mM KCl each had a scattering intensity approximately 0.05. The scattering signal increased steeply to roughly 0.9 when Lys_{18} was added to 50 μM, prior to additions of the nucleotides

filaments were dispersed by the treatment with ATP, and appeared similar to images obtained from control experiments on fd and F-actin suspensions without adding any bundling agent (not shown). The striking effect of ATP confirms our light scattering measurements, and the similar behavior between these two systems agrees with the nonspecific electrostatic model.

A close comparison of electron microscopic images of fd and F-actin reveals interesting differences between these two systems. First, although individual F-actin and fd filaments appear to have roughly the same diameter, fd appears much more flexible on the EM picture. There appear to be more bends and branches in fd bundles as well. This comparison is interesting since the persistence length of fd is reportedly about 2200 nm [27, 28], while the reported persistence length of F-actin varies from 2 to above 10 μm in the literature [29, 30]. Secondly, many areas of F-actin bundles show a common striation pattern along the filament axis, some noted by arrows on the electron micrograph (a). The striations have a periodicity of approximately 36 nm, corresponding to the helical structure of F-actin. Our EM images also suggest that most of the F-actin helices tend to axially align when bundled by $Co(NH_3)_6^{3+}$. This type of alignment has been previously characterized for actin bundles among many possible forms of paracrystalline structures [31]. fd bundles, however, appeared rather loose, without apparent pattern of striations.

3.2 Effect of the Polyelectrolyte Concentration

Cation-induced bundling of the four biopolymers described here is largely independent of the concentration of the negatively charged macromolecules. The concentration of $Co(NH_3)_6^{3+}$ required for an abrupt increase in light scattering was approximately constant for F-actin over a concentration range from 0.1 – 6.0 mg/ml (2.4 – 144 μM). In

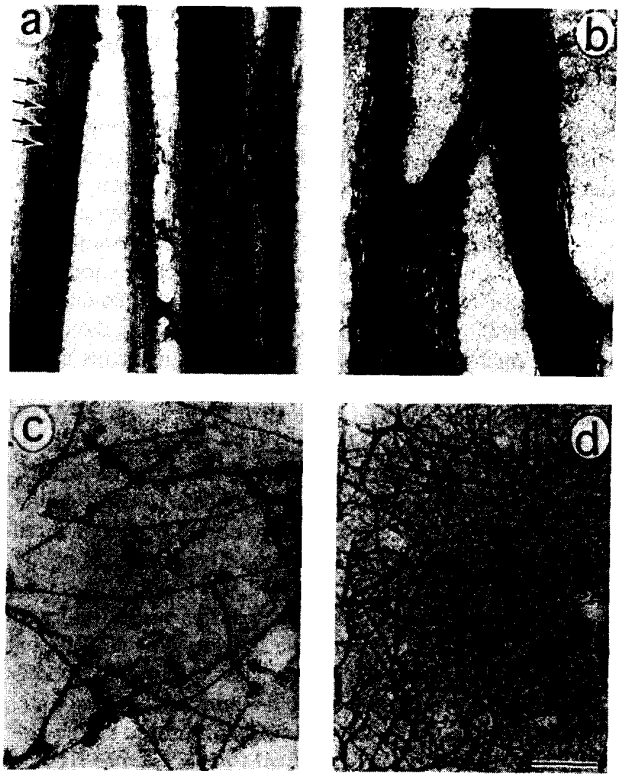

Fig. 3
Electron micrographs of negatively stained F-actin (a and c) and fd (b and d) in the presence of 5 mM $Co(NH_3)_6^{3+}$, prior to (a, b) and after (c, d) the addition of 5 mM ATP. The scale bar represents 100 nm in (a) and (b), and 200 nm in (c) and (d). Arrows in (a) point to striations of 36 nm periodicity, one of the characteristic morphologies for actin bundles

this case, the concentration of free $Co(NH_3)_6^{3+}$ required for bundling is in the order of millimolar, and therefore the micromolar amounts of $Co(NH_3)_6^{3+}$ that the F-actin surface recruits as counterions are negligible. However, the situation becomes different when the bundles are induced by polyvalent cations of much higher apparent binding affinity to the macromolecules. For instance, when only micromolar free polycations are required to induce bundles, as is the case for Lys_{18} and MT, the total added amount of the polycations required for bundle formation may appear to vary linearly with the concentration of the macromolecules. Rather than implying a specific binding site on microtubules for polylysine, this apparent stoichiometry occurs simply because polycations recruited to the condensation zone of the microtubules correspond to a fixed portion of their total surface charge and therefore are proportional to their concentration.

Fig. 4 shows the measurements of light scattering change for MT of 3 concentrations: 0.1, 0.3, and 0.9 mg/ml. The onset concentration of Lys_{18} was visually determined from 4(a), and plotted vs. the molar concentration of tubulin heterodimers. The linear fit extrapolates to 1.62 μM at the

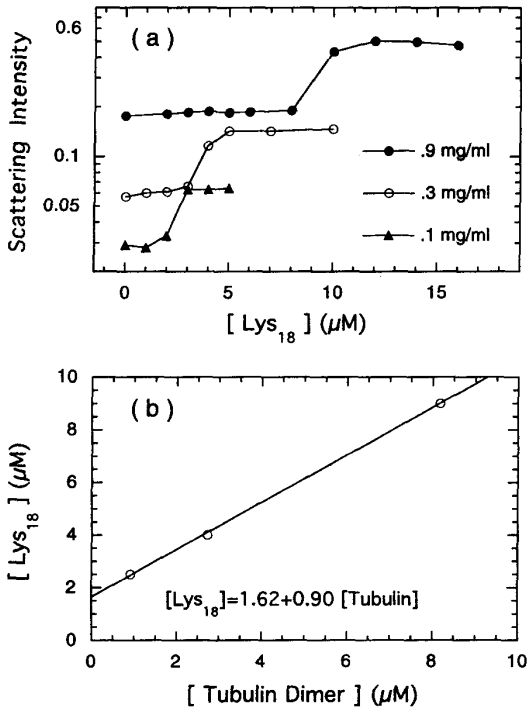

Fig. 4
(a) Light scattering measurements of microtubule suspensions at three concentrations, following sequential additions of Lys_{18}. The concentration of Lys_{18} corresponding to a sharp increase in scattering on each plot was visually determined, and it was plotted in (b) as a function of tubulin concentration. The result of a linear fit is shown

vertical axis, corresponding to the threshold concentration of [Lys_{18}] for a trace amount of MTs to bundle, while the slope value of 0.9 indicates less than one Lys_{18} molecule was restricted to near the MT surface per one tubulin dimer. Note although one tubulin dimer carries nearly 50 net negative charges based on counting the charged amino-acids, a charge balance between these two species does not hold. Instead, excess amounts of monovalent cations and anions ensure the neutrality of the entire region.

3.3 Dependence on the Filament Length

F-actin is an ideal system to test the effect of filament length on the bundle formation. This is largely due to the existence of gelsolin, an efficient actin severing protein of 82 kD molecular weight. When polymerized in the absence of gelsolin, F-actin may grow to well above 10 μm, yet the filaments remain extended and have only moderate bending curvatures. Each gelsolin molecule is capable of severing an actin filament. It then binds to and caps the primary growth end, noted as the barbed or plus end of F-actin. With the plus end capped, the treadmilling process of F-actin stops, and eventually the suspension reaches an equilibrium length distribution. The filaments remain polydisperse in length as is the case without gelsolin, and the length distribution has been characterized to be exponential [32]. We found however that the bundle formation mechanism has little to do with these complications, including polydispersity, polarity of the filaments, and the binding of a small ratio of gelsolin. This property allows a systematic test of a possible length dependence for bundling of actin by polycations, by varying the ratio of actin to gelsolin.

Fig. 5 shows the light scattering increases caused by adding Lys_{18} into 0.2 mg/ml F-actin solutions with different lengths determined by various amounts of gelsolin. The onset bundling profile varies very little until the filaments are shortened to contain only 50 monomers (140 nm) on average. This finding confirms that the basic prediction of charge condensation is applicable to cylindrical filaments of sufficiently large aspect ratios (>20:1). EM of these samples detects aggregates that are of comparable sizes, but are shorter along the filament axis and slightly wider laterally when formed from shorter filaments (not shown). These results therefore suggest that the infinite length of filaments is a mathematical simplification in the counterion condensation theory, rather than a strict requirement in predicting the lateral association.

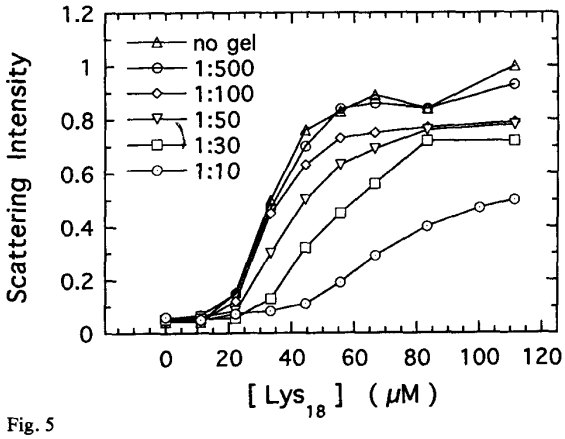

Fig. 5
Comparison of the bundle formations of F-actin of various lengths. Actin concentration was 0.2 mg/ml for all the samples, with different gelsolin: actin ratio as noted in the figure

3.4 Apparent Binding Affinity as a Function of Ionic Strength

Monovalent ions are often abundant in solutions of polyelectrolytes. Their effect on the apparent binding of polyvalent counterions to the charged macromolecular surface has been a natural aspect of counterion condensation theory. We demonstrate in this section that such effects of monovalent salt can be probed through the light scattering measurements of bundle formations.

Fig. 6 shows a series of light scattering measurements to illustrate the extreme sensitivity of bundle formation as a function of ionic strength. First, concentrated $Co(NH_3)_6^{3+}$ was added into 0.1 mg/ml fd virus in 5 mM Tris buffer at pH 7.5, 1 mM NaN_3, and no KCl. The solution ionic

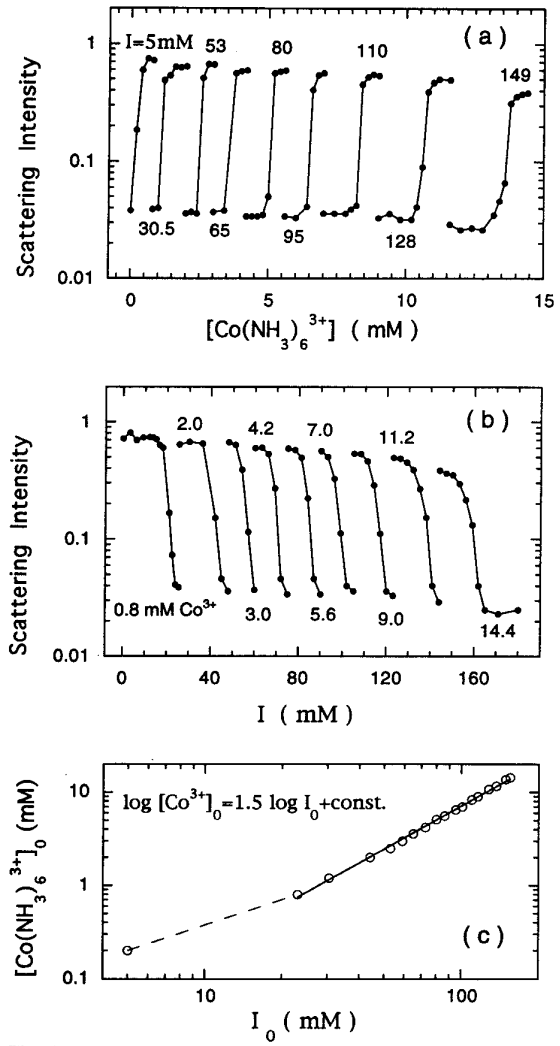

Fig. 6
(a) 0.1 mg/ml fd in solution of initial ionic strength approximately 5 mM was subject to addition of $Co(NH_3)_6^{3+}$, until the scattering intensity saturates at a high level. (b) Concentrated KCl was added in order to increase the solution ionic strength until the scattering signal drops to the low level, corresponding to dissolution of fd bundles. This process was repeated for a total of nine cycles. (c) Relationship between $Co(NH_3)_6^{3+}$ and the solution ionic strength. The data were determined from (a) and (b). A power law formula was applied to the data at above 20 mM ionic strength and the results shown above the plot. Co^{3+} on (b) and (c) is a short note for $Co(NH_3)_6^{3+}$

strength is calculated to be 5 mM, considering roughly 80% of Tris in the dissociated form [17]. In such condition of low ionic strength, 0.5 mM $Co(NH_3)_6^{3+}$ induced a steep increase in light scattering, indicating fd bundle formation (Fig. 6a). The scattering intensity saturated with 0.75 mM $Co(NH_3)_6^{3+}$, and then KCl was sequentially added into the solution (Fig. 6b). The scattering intensity decreased sharply when the concentration of KCl rose to about 20 mM, indicating dissolution of bundles. The disaggregation of fd bundles seemed complete at about 25 mM KCl, since the scattering intensity dropped to the initial level when no $Co(NH_3)_6^{3+}$ was added into the solution. We then switched to additions of $Co(NH_3)_6^{3+}$ again, shown as the second curve from the left on Fig. 6a. This process continued for a total of nine cycles, shown in 6a and b. Note in a and b the scattering readings at both the high and lower plateau tend to decrease, because of the increasing coloration from the excess $Co(NH_3)_6^{3+}$ ions. A control test of adding $Co(NH_3)_6^{3+}$ into a cuvette of water cause a similar progressive reduction of the light scattering signal.

From Fig. 6a, each region of sharp change in scattering locates a critical conditions in which a threshold population of $Co(NH_3)_6^{3+}$ ions condense to the immediate surroundings of fd filaments. At such a condition, the attractive interaction due to $Co(NH_3)_6^{3+}$ has just reached a balance with the interfilament repulsion, and lateral aggregates start to form. By defining the point at which light scattering first rises steeply from its baseline, a value for the $Co(NH_3)_6^{3+}$ concentration required to induce bundles at a given ionic strength was obtained. From here on, a subscript "0" is noted whenever a concentration is quoted from the onset bundling conditions, such as $[Co(NH_3)_6^{3+}]_0$ and the corresponding ionic strength I_0. Likewise, another pair of values of $[Co(NH_3)_6^{3+}]_0$ and I_0 was extracted from one descending curve in Fig. 6b, by defining a value at which the light scattering first decreases steeply. These values were put together and plotted in 6c. The data obtained from Fig 6a and b fit rather well into one curve, suggesting strongly that these data points correspond to the same equilibrium conditions. Overall, the data obtained above 20 mM ionic strength fit very well to a power law relationship, $[Co(NH_3)_6^{3+}]_0 \propto I_0^{1.5}$.

In order to understand the power law relationship between $[Co(NH_3)_6^{3+}]_0$ and I_0, we first apply the simplest Manning theory of apparent binding. Manning theory predicts a counterion condensation zone whose volume is independent of solution ionic strength. If one further assumes that the lateral association occurs when a fixed percentage of the charge on the polyelectrolytes is neutralized, independent of the solution ionic strength, one would conclude that a fixed local concentration of $[Co(NH_3)_6^{3+}]_{loc}$ and a complementary concentration of monovalent cations $[K^+]_{loc}$ are expected at the onset bundling conditions. The association constant for the apparent binding of $Co(NH_3)_6^{3+}$ to polyelectrolyte surface, defined as $K_n = [Co(NH_3)_6^{3+}]_{loc}/[Co(NH_3)_6^{3+}]_{free}$, is therefore inversely proportional to $[Co(NH_3)_6^{3+}]_0$ as free ions in solution. As discussed earlier in section 3.2, since the amount of counterion recruited to the macromolecule surface can be neglected, $[Co(NH_3)_6^{3+}]_0$ is roughly the concentration of total added $Co(NH_3)_6^{3+}$.

The Manning one-variable theory predicts the following relations [2]:

i) in the range that $\theta_N \leq N^{-1}(1-\xi^{-1})$, $d \log K_N / d \log I = -N$, where I is ionic strength, and $N = 3$ for $Co(NH_3)_6^{3+}$. This relation leads to $\log [Co(NH_3)_6^{3+}]_0 = 3 \log I_0 + \text{const}$, which does not agree very well with our experiment.

ii) If $N^{-1}(1-\xi^{-1}) < \theta_N \leq N^{-1}(1-N^{-1}\xi^{-1}$, then $d \log K_N / d \log I = -N\xi(1-N\theta_N)$, which varies between 1 and N. Putting the experimental result of 1.5 into the above

expression, one would obtain $\theta_3 = 0.95/3$, suggesting that 95% of fd surface charge is neutralized by $Co(NH_3)_6^{3+}$ when bundles form.

In the case of charged cylinders, it has been later derived that the thickness of the condensation layer is proportional to $\kappa^{-1/2}$, instead of being independent of ionic strength [6, 8]. Let us still assume a criterion for bundle formation such that the charged surface is neutralized to a fixed portion of the surface charge by the counterions in the condensed layer, even though the thickness of counterion layer varies with I. Now the local concentration of the trivalent cobalt ions is related to the ionic strength as follows, $[Co(NH_3)_6^{3+}]_{loc} \propto 1/\kappa^{-1/2} \propto 1/I^{-1/4}$. In conjunction with the experimental relation $\log [Co(NH_3)_6^{3+}]_0 \propto 1.5 \log I_0$, one would obtain $d \log K_N / d \log I = 1.75$ and a slightly different fraction of the condensed cobalt ion $\theta_3 = 0.94/3$. If one simply assumes the thickness of the condensation layer to be proportional to the Debye screening length κ^{-1}, a similar derivation would obtain $d \log K_N / d \log I = -2$ and $\theta_3 = 0.93/3$. The actual value determined here bears little significance because of a number of simplifications in the above treatments. However, the theoretical prediction of a power law dependence agrees very well with our experimental data.

3.5 Macromolecules as an Indicator of Ion Cluster Formations

In Fig. 2, it has been shown that fd bundles induced by Lys_{18} can be disaggregated by the polyanionic nucleotides. We proposed that this is due to the interaction between Lys_{18} and AP5A, ATP, ADP, or AMP. By analysis of such an interaction, one can derive the association constants of a variety of polycation-polyanion clusters through our model.

We first measured the onset concentration of $Co(NH_3)_6^{3+}$ at which 0.1 mg/ml fd in 50 mM KCl forms bundles. This onset concentration was located when a steep increase occured as shown in Fig. 1b, although the curve there was measured for a sample concentration of 0.3 mg/ml. Then ATP was sequentially added until the fd bundles completely dissolved, and the $[ATP]_0$ that corresponds to the balancing bundling condition at 1.8 mM $Co(NH_3)_6^{3+}$ was located. This process was continued through many cycles, much as the case of varying ionic strength shown in Fig. 6a and b. The actual curves of light scattering intensities are not shown, but instead we plot the concentration $[Co(NH_3)_6^{3+}]_0$ required for bundling as a function of $[ATP]_0$ in Fig. 7a. The data fit well to an expression derived in the appendix, assuming ATP and $Co(NH_3)_6^{3+}$ form the following clusters,

$$4\,Co(NH_3)_6^{3+} + 3\,ATP = [Co(NH_3)_6^{3+}]_4ATP_3$$

The fit of data to the formula $[ATP]_0 = (3/4)\{[Co(NH_3)_6^{3+}]_0 - m_1\} + m_2\{[Co(NH_3)_6^{3+}]_0 - m_1\}^{1/3}$ determines $m_1 = 1.1$ mM, $m_2 = 0.343$ $(mM)^{2/3}$. m_1 is the free $[Co(NH_3)_6^{3+}]$ required for fd bundle formation at 50 mM KCl. From the value of m_2, we obtain the dissociation constant $K = 0.24$ $(mM)^6$.

A strict charge balance is not required in the above expression, although ATP is known to carry 4 negative phosphate charges. In addition to ATP and $Co(NH_3)_6^{3+}$, there is an excess amount of monovalent ions that may also participate in the cluster formation, as do water molecules. However, these effects are not dealt with here, based on the simple argument that interactions between polyvalent charges ought be much stronger. The ratio 4:3 was chosen because it produced an excellent fit. A separate fit with this ratio as an additional parameter gave a coefficient close to 0.7 as opposed to the value of 0.75 assumed in the current fit.

In order to test further the concept of ion cluster formation, and to show it is independent of the species of macromolecules tested, an identical experiment was performed with a 0.5 mg/ml F-actin solution in 150 mM KCl. The results are shown in Fig. 7b. A curve fit with the same formula again agrees well with experimental data. 2.76 mM of $Co(NH_3)_6^{3+}$ is determined as the onset bundling concentration in absence of ATP, and the dissociation constant for the $[Co(NH_3)_6^{3+}]_4ATP_3$ complex is calculated to be 290 $(mM)^6$ at 150 mM KCl. Although in the present case

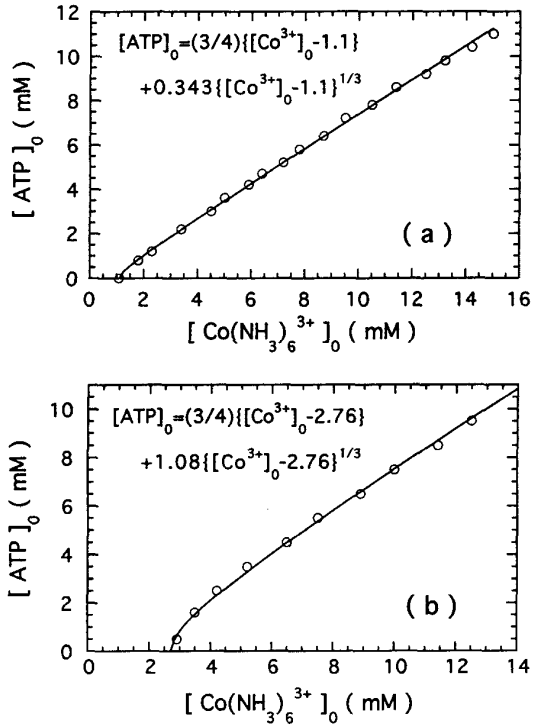

Fig. 7
(a) ATP concentration in a suspension of 0.1 mg/ml fd in 50 mM KCl as a function of $[Co(NH_3)_6^{3+}]_0$, at the onset bundling conditions. Each data point was determined following a series of additions of either concentrated ATP or $Co(NH_3)_6^{3+}$, as demonstrated in Fig. 6. A formula fit result is shown on the plot, based on the association between $4\,Co(NH_3)_6^{3+}$ and 3 ATP ions. (b) Identical experiment with 0.5 mg/ml F-actin at 150 mM KCl

both ionic strength and the nature of the polyelectrolyte were different in the two sets of measurements, these data illustrate how the ionic strength dependence of polyion cluster formation can be determined. Comparison with the K value at 50 mM KCl reveals an increase in apparent dissociation constant by roughly a thousand fold with a three fold increase of ionic strength.

The formation of ion clusters between polylysine and ATP was tested as another example. Since the homopolymer of lysine used is much larger than an ATP molecule, we assume that formation of one cluster involves only one lysine polymer and a few molecules of ATP, i.e.

$$Lys_{18} + n\,ATP = Lys_{18}(ATP)_n$$

The formula $[ATP]_0 = n\{[Lys_{18}]_0 - m_1\} + m_2\{[Lys_{18}]_0 - m_1\}^{1/n}$ was applied, and the excellent fit shown in Fig. 8 seems to support the above assumption of single polymer involvement. The three fit values obtained were: $m_1 = 0.019$ mM, $m_2 = 4.56$, and $n = 4.4$. The non-integral value of n is probably the result of incomplete ionization or an unknown degree of polydispersity in the commercial preparation of lysine eighteenmers. However, the number 4.4 is close to the ratio between the numbers of charges which polylysine and ATP each carry, suggesting an approximate charge balance without much involvement of monovalent ions.

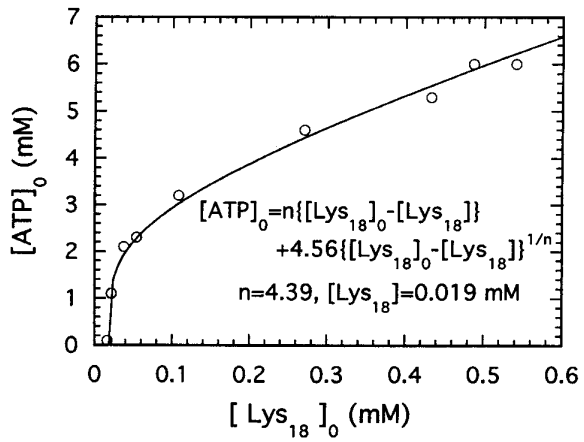

Fig. 8
ATP level at the onset condition of bundle formation as a function of $[Lys_{18}]_0$. The solution initially contained 0.4 mg/ml F-actin at 150 mM KCl. The fit formula assumes the cluster formation between one polycationic Lys_{18} and n ATP ions, and the results are shown on the figure

4. Discussion

Although counterion condensation has been a subject of extensive study, previous application to biological systems has been largely limited to explain DNA condensation. Up to this report, no similar physical mechanism based on such a simple analogy has been proposed for the bundle formation of F-actin, MT, fd, or TMV. Our experiments not only demonstrate the lateral formation of these charged biopolymers, but also present this class of formations as a natural consequence of counterion condensation phenomena.

Our model of cation induced lateral association results in a number of predictions. First, the formation requires polyvalent counterions, including divalent counterions in some cases. Counterions of higher valence generally induce bundle formation at lower concentrations. Differences between counterions of the same valence are not expected to be too great, and these differences should not depend on the individual polyelectrolytes. Second, bundle formation does not cause irreversible changes in the internal structure of polymer filaments. The process may be reversed either by adding monovalent salt to increase ionic strength, or adding polyvalent coions to reduce the concentration of free counterions. Third, the formation does not depend on the concentration of macromolecules, but rather it is crucial how much free polyvalent counterions are present in solution.

Bundle formation by rodlike polyelectrolytes generally involves attractive interactions between the neighboring filaments. This property distinguishes it from another type of bundling process, namely the formation of a liquid crystalline phase. Onsager illustrated in 1949 [33] through a statistical mechanical treatment that rodlike particles, neutral or charged, may form orientationally ordered phases. The orientational order does not require attractive interactions, but instead the formation is caused by the excluded volume effect, and it requires a threshold concentration of the rodlike particles. In contrast to counterion-induced bundling, the onset concentration for liquid crystalline formation is inversely proportional to the length of the particles in suspension.

Flory later derived the same liquid crystalline formation for semiflexible polymers, based on a lattice model [34]. The Flory prediction of isotropic-nematic transition depends on an interaction parameter χ, which varies from negative to positive. $\chi = 0$ corresponds to no interaction. Flory theory has been widely applied to liquid crystalline formation of synthetic polymers, but the formation of liquid crystalline phase of DNA can also be attributed to an attractive interaction, induced for example by spermidine [35]. However, an attractive interaction is not required in general to explain the liquid crystalline formation which has also been observed for all the four biopolymers studied in this report. We conclude that bundle formation by condensed counterions and orientational ordering in the liquid crystalline phase are two distinct processes, despite the superficial similarity of the lateral arrays of filaments they produce.

The fd virus is perhaps an ideal model to study in order to obtain quantitative comparison with polyelectrolyte theories. Each virus is coated by about 2800 identical protein subunits, with a five fold rotation axis and an approximate two fold screw axis [36, 37]. The virus has a high linear charge density of roughly -10 e/nm at pH 7.3, and the negative charges are uniformly distributed on the virion. The most simplified Manning counterion condensation theory predicts that counterions of approximately 86% of the surface charges are confined in a thin layer in

monovalent electrolyte, and 93% so when sufficient divalent cations are present. We find experimentally in Fig. 1 that for divalent metal ions, concentrations of tens of millimolar are required, suggesting that over 90% of charge neutralization is required for the bundle formation to occur. This prediction also agrees with the criterion for bundle formation induce by millimolar $Co(NH_3)_6^{3+}$, in which case a simplified one-variable treatment predicts 94% charge neutralization.

The measurements of bundle formation of fd as a function of ionic strength, shown in Fig. 6, provide a possibility for quantitative testing of theoretical calculations for cylindrical polyelectrolytes. Based on the simplified Manning one-variable treatment, we were able to explain the power law dependence between the onset concentration of the polycation used, $Co(NH_3)_6^{3+}$, and the concentration of the monovalent salt. The dependence seems to deviate significantly from the power law behavior at low ionic strength. We speculate that theoretical modification must be considered since the situation is more complicated at low ionic strength, perhaps due to more extensive lateral redistribution of the counterion clouds. Detailed further experiments at very low ionic strength may provide additional information.

The concept of ion cluster formation of polyvalent cations and anions explains the experimental data shown in Figs. 7 and 8. Our treatment is based on the crucial assumption that the onset of bundling corresponds to a fixed concentration of polyvalent counterions in the fully dissociated form. This assumption is more justifiable than a similar one postulated earlier (Sect. 3.4) in dealing with the dependence on ionic strength. In describing Fig. 6a, a fixed portion of the counterion charge was assumed to be required for the lateral association to occur, despite the variation in ionic strength. In the case of adding polyvalent counterions/coions, however, solution ionic strength is nearly constant at the onset of bundling. There is also ample space in solution for the polyvalent coions to reside, hence there remains a negligible fraction of polyvalent coions close to the biopolymer surface.

Reversible lateral associations of biopolymers play significant structural and functional roles in cellular systems. Large stress fibers in the cytoskeleton, filopodia and lammellipodia at the cell front, and large neuronal cores are but a few examples of bundled structures in cells. Although numerous proteins facilitate the formation of bundles of F-actin and MT, it is unclear in many cases whether these proteins contain dual binding sites or if they are the sole regulators of the assembly process. Our suggestion of a general electrostatic interaction may provide a new integrated approach toward understanding a number of biological processes.

We thank S. Fraden and D.L.D. Caspar for access to TMV and fd phage, and for helpful discussions with them. We thank Rolands Vegners for providing the lysine and histidine oligomers. We appreciate assistance from J.H. Hartwig, J. Kas, and P.G. Allen. We also thank G. Manning for his encouragement. This work was supported by NIH grants AR38910 and HL19429.

Appendix

We are interested in the general cluster formation between polycation A and polyanion B in a solution of excess monovalent salt:

$$mA + nB = A_mB_n \tag{1}$$

This formation has a dissociation constant

$$K = [A]^m[B]^n/[A_mB_n] \ . \tag{2}$$

The analysis is simplified by assuming that conditions are reached where the concentration of free polycations is constant. We then seek a relationship between the total concentrations $[A]_0$ and $[B]_0$ that satisfy these conditions which are detected by the bundling of the polyelectrolyte. Since $[A]_0 = [A] + m[A_mB_n]$ and $[B]_0 = [B] + n[A_mB_n]$, we first obtain the following expressions $[A_mB_n] = ([A]_0 - [A])/m$, and $[B] = [B]_0 - n[A_mB_n] = [B]_0 - (n/m)([A_0] - [A])$. Substituting into equation (2),

$$K = \frac{[A]^m[B]^n}{[A_mB_n]} = \frac{[A]^m\{[B]_0 - \frac{n}{m}([A]_0 - [A])\}^n}{([A]_0 - [A])/m}$$

we obtain

$$[B]_0 = \frac{n}{m}([A]_0 - [A]) + \left(\frac{K}{m[A]^m}\right)^{1/n}([A]_0 - [A])^{1/n} \ . \tag{3}$$

References

[1] V.A. Bloomfield, Biopolymers *31*, 1471 – 1481 (1991).
[2] G.S. Manning, Quarterly Rev. Biophys. *II*, 179 – 246 (1978).
[3] R. Marquet and C. Houssier, J. Biomol. Struct. Dyn. *9*, 159 – 167 (1991).
[4] J. Ray and G.S. Manning, Langmuir *10*, 2450 – 2461 (1994).
[5] F. Oosawa, Polyelectrolytes, Marcel Dekker, Inc., 1971.
[6] M. Le Bret and B.H. Zimm, Biopolymers *23*, 287 – 312 (1984).
[7] K.S. Schmitz, Macroions in Solution and Colloidal Suspension, VCH, New York, 1993.
[8] M. Le Bret and B.H. Zimm, Biopolymers *23*, 271 – 285 (1984).
[9] J.E. Sanchez-Sanchez and M. Lozada-Cassou, Chem. Phys. Lett. *190*, 202 – 208 (1992).
[10] T.P. Stossel, Science *260*, 1086 – 1094 (1993).
[11] P.M.G. Curmi, J.A. Barden, and C.G.D. Remedios, J. Mus. Res. Cell Mot. *5*, 423 – 430 (1984).
[12] H. Strzelecka-Golaszewska, E. Prochniewicz, and W. Drabikowski, Eur. J. Biochem. *88*, 229 – 237 (1978).
[13] N.J. Grant, C. Oriol-Audit, and M.J. Dickens, Eur. J. Cell Biol. *30*, 67 – 73 (1983).
[14] W.E. Fowler and U. Aebi, J. Cell Biol. *93*, 452 – 458 (1982).
[15] C. Oriol-Audit, M.W. Hosseini, and J. Lehn, Eur. J. Biochem. *151*, 557 – 559 (1985).
[16] S. Fraden, G. Maret, D.L.D. Caspar, and R.B. Meyer, Phys. Rev. Lett. *63*, 2068 – 2071 (1989).
[17] J.X. Tang and S. Fraden, Liquid Crystals *19*, 459 – 467 (1995).
[18] B.M. Millman, T.C. Irving, B.G. Nickel, and M.E. Loosley-Millman, Biophys. J. *45*, 551 – 556 (1984).
[19] V.A. Parsegian and S.L. Brenner, Nature *259*, 632 (1974).
[20] J. Spudich and S. Watt, J. Biol. Chem. *246*, 4866 – 4871 (1971).
[21] W.A. Voter and H.P. Erickson, J. Biol. Chem. *256*, 10430 – 10438 (1984).
[22] D.L.D. Caspar, Adv. Protein Chem. *18*, 37 (1963).
[23] J. Sambrook, E.F. Fritsch, and T. Maniatis, Molecular Cloning: A Laboratory Manual, *1*, Cold Spring Harbor Lab Press, 1989.
[24] H. Kurokawa, W. Fujii, K. Ohmi, T. Sakurai, and Y. Nonomura, Biochem. Biophys. Res. Commun. *168*, 451 – 457 (1990).
[25] R.C. Weisenberg, Science *177*, 1104 – 1105 (1972).

[26] J. Kolakowski, R. Makuch, D. Stepkowski, and R. Dabrowska, Biochem. J. (1995).
[27] E. Loh, E. Ralston, and V.N. Schumaker, Biopolymers *18*, 2549, and 2569 (1979).
[28] L. Song, U.-S. Kim, J. Wilcoxon, and J.M. Schurr, Biopolymers *31*, 547 – 567 (1991).
[29] H. Isambert et al., J. Biol. Chem. *270*, 11437 – 11444 (1995).
[30] J. Kas, H. Strey, and E. Sackmann, Nature *368*, 226 – 229 (1994).
[31] C.H. Owen, D.J. DeRosier, and J. Condeelis, J. Struct. Biol. *109*, 248 – 254 (1992).
[32] P.A. Janmey, J. Peetermans, K.S. Zaner, T.P. Stossel, and T. Tanaka, J. Biol. Chem. *261*, 8357 – 8362 (1986).
[33] L. Onsager, Ann. NY Acad. Sci. *51*, 627 – 659 (1949).
[34] P.J. Flory, Statistical Mechanics of Chain Molecules, Interscience Publishers, 1969.
[35] J.-L. Sikorav, J. Pelta, and F. Livolant, Biophys. J. *67*, 1387 – 1392 (1994).
[36] L.A. Day, C. J. Marzec, S.A. Reisberg, and A. Casadevall, DNA Packing in Filamentous Bacteriophages. Ann. Rev. Biophys. Chem. *17*, 1988.
[37] L. Makowski, Virus Structures, Biological Macromolecules and Assemblies, *1*, 1984.

Presented at the First International Symposium on Polyelectrolytes and Discussion Meeting of the Deutsche Bunsen-Gesellschaft für Physikalische Chemie "Polyelectrolytes in Solution and at Interfaces" in Potsdam, September 18th to September 22nd, 1995

E 9143